

Skin-Inspired, Fully Autonomous Self-Warning and Self-Repairing Polymeric Material under Damaging Events

He Zhang,^{*,†,‡,§} Xin Zhang,[§] Chenlu Bao,^{||} Xin Li,[⊥] Fei Duan,[#] Klaus Friedrich,[▽] and Jinglei Yang^{*,||,¶}

[†]National Engineering Research Center of Novel Equipment for Polymer Processing, Key Laboratory of Polymer Processing Engineering (SCUT), Ministry of Education, South China University of Technology, Guangzhou, 510641, China

[‡]Guangdong Provincial Key Laboratory of Technique and Equipment for Macromolecular Advanced Manufacturing, South China University of Technology, Guangzhou, 510641, China

[§]School of Civil and Environmental Engineering, Nanyang Technological University, 639798, Singapore

^{||}School of Materials Science and Engineering, Tianjin Polytechnic University, Tianjin, 300387, China

[⊥]National Laboratory of Solid State Microstructures and Department of Materials Science and Engineering, Nanjing University, Nanjing 210093, China

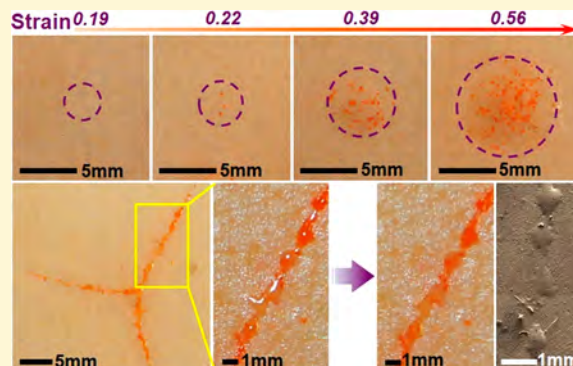
[#]School of Mechanical and Aerospace Engineering, Nanyang Technological University, 639798, Singapore

[▽]Institute for Composite Materials, Technical University of Kaiserslautern, Kaiserslautern, D-67663, Germany

[¶]Department of Mechanical and Aerospace Engineering, The Hong Kong University of Science and Technology, Kowloon, Hong Kong SAR

Supporting Information

ABSTRACT: Polymers are susceptible to small damage which is difficult to detect and repair and may lead to catastrophic failure if left unattended at the early stage. How to autonomously warn and repair the damage simultaneously is a promising yet challenging task, owing to the difficulty in integrating different functional elements for packaging and lack of suitable vehicles to carry a multirole trigger with high reactivity. Herein, inspired by human skin in the damage-healing process, we report a genuinely fully autonomous smart material that is capable of warning of and healing damage via simply incorporating dual microcapsules containing polyamine as a multirole trigger and epoxy monomer dyed with a pH indicator, respectively. Both microscopic “subcutaneous” damage and macroscopic surface damage can be warned of by a conspicuous red color, not only rapidly upon occurrence but also permanently after being repaired. Accompanied with the comprehensive warning, the smart material shows high healing performance upon dynamic impact damage with efficiency up to 100% without external interventions. This facile and ready strategy with fully autonomous warning and healing functions independent of the host matrix provides a new avenue to enhance the reliability and longevity of a wide variety of polymeric materials ranging from functional coatings to structural composites.



INTRODUCTION

Smart material that can respond autonomously to damage is highly demanded to increase safety and extend the lifespan of the servicing materials.^{1–5} To date, diverse related functions have been proved, at least conceptually, to verify their feasibility, including self-protection,^{6–10} self-sensing,^{11–13} self-reporting,^{14–17} self-healing,^{18–27} etc. Besides exploring new functions, one trend of developing smart materials is to integrate as many different functions as possible into the same matrix to comprehensively protect the material.^{28–35} However, incorporation of multifunction via a simple addition of monofunctional motifs could inevitably increase a material's complexity exponentially during their synthesis, processing,

and maintenance. Thus, how to integrate different functions into less functional carriers is crucial to fabricate practical smart materials.

For integrating multifunction, nature has taught us much and could still share with us more. After evolution for thousands of years, a creature has combined and optimized their organs to realize required maximum functions with minimum sources, such as human skin. By only the distributed blood vessels alone to deliver different functional substances, it

Received: January 27, 2019

Revised: March 15, 2019

Published: March 18, 2019

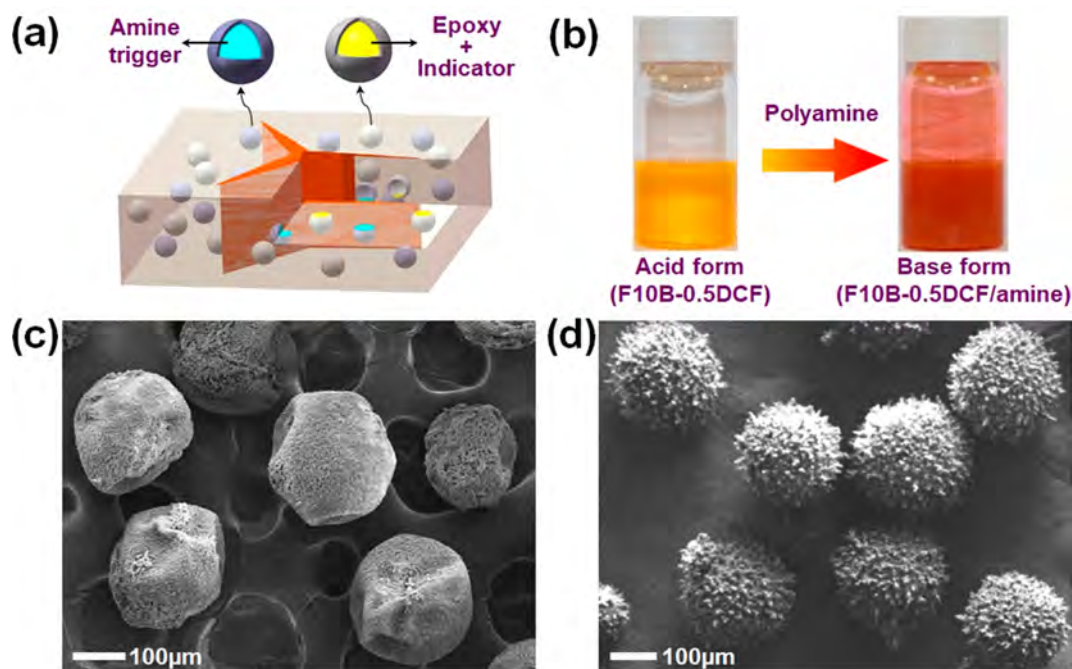


Figure 1. (a) Scheme of the skin-inspired smart material with capability of warning and repairing damage. (b) Rapid color change of F10B-0.5DCF with the presence of 1–2 droplets of 25TEPA75T403 for self-warning function. (c) Adopted 25TEPA75T403 microcapsules. (d) Adopted F10B-0.5DCF microcapsules.

is able to autonomously warn of and heal injuries, including bruising for microscopic subcutaneous injuries, reporting and healing macroscopic wounds by bleeding, and finally recording the healed serious injuries by scarring. Inspired by this, smart materials were explored to fully or partially simulate these functions via color indication and/or self-healing.^{28–31,33} While color can visualize damage to warn of the vulnerability of the damaged area and prevent further damage to the same site, self-healing can restore the degraded properties to retard or even avoid material failure for enhanced safety and longevity. Feasibility of fabricating polymeric materials with dual functions was explored through possible incorporation of vehicles containing color indicator and healant.^{28–31,33} Synthetic materials that are able to visualize damage with the aid of an extra UV source and autonomously repair damage were achieved by using extrinsic carriers with both healants and fluorescein.^{28,29,32,34} However, they are passive reporting systems in that the color is always on in both the damaged and the intact sites, leading to the low contrast and therefore less effectiveness for damage indication. Although active reporting systems, in which color for warning was only triggered upon occurrence of damage, was illustrated conceptually based on hollow tubes or microcapsules,^{31,33} none of them are genuinely autonomous for the self-healing function since external interventions, such as thermal treatment or manual addition of healant, are necessary due to the lack of suitable vehicles to carry substances with high reactivity.

To develop this kind of smart material, the core problems are how to reasonably combine suitable functional elements with high activity and how to explore the right approaches to package the designed combinations. As a color indicator for warning can be mixed and encapsulated with healant,³¹ the bottleneck is how to package a multirole trigger that can activate rapid and evident color change and at the same time solidify healants autonomously without external interventions.

In the prior art, we successfully fabricated microcapsules containing pure polyamine, which has the potential to act as both an alkaline trigger of pH indicators for color indication and a hardener of epoxy monomer or diisocyanate for self-healing.³⁶ Herein, inspired by human skin, we report for the first time a fully autonomous multifunctional system that enables comprehensive warning of damage at different levels and stages and simultaneously autonomous healing of damage with high performance via simply incorporating dual microcapsules containing polyamine and epoxy monomer dyed with a pH indicator, respectively (Figure 1a).

RESULTS AND DISCUSSION

Design of the Smart Material. This smart system was carefully designed to consider both fast visualization and autonomous repair of damage at room temperature (RT ~ 22–25 °C) without any external intervention. A highly reactive amine mixture, i.e., 25 wt % tetraethylenepentamine and 75 wt % JEFFAMINE T403 (25TEPA75T403), was selected as the multirole trigger, and an epoxy mixture, i.e., bisphenol F diglycidyl ether diluted by 10 wt % butyl glycidyl ether (F10B), and a pH indicator, i.e., 2',7'-dihydrochlorofluorescein (DCF), were chosen as the healant and color indicator to achieve the self-healing and self-warning functions. They were adopted because 25TEPA75T403 is capable of not only curing F10B with high performance to enable full recovery of mode I fracture toughness for epoxy matrices³⁶ but also triggering rapid and evident color change of DCF. The epoxy mixture (F10B) dyed with a low concentration (0.5 wt %) of DCF, namely, F10B-0.5DCF, is highly sensitive to 25TEPA75T403 and changes immediately from bright yellow to conspicuous red upon addition of 1–2 droplets of the amine mixture (Figure 1b). 25TEPA75T403 was encapsulated following a protocol by integrating microfluidic emulsion and interfacial polymerization (Figure 1c, $249 \pm 42 \mu\text{m}$),³⁶ while F10B-0.5DCF was

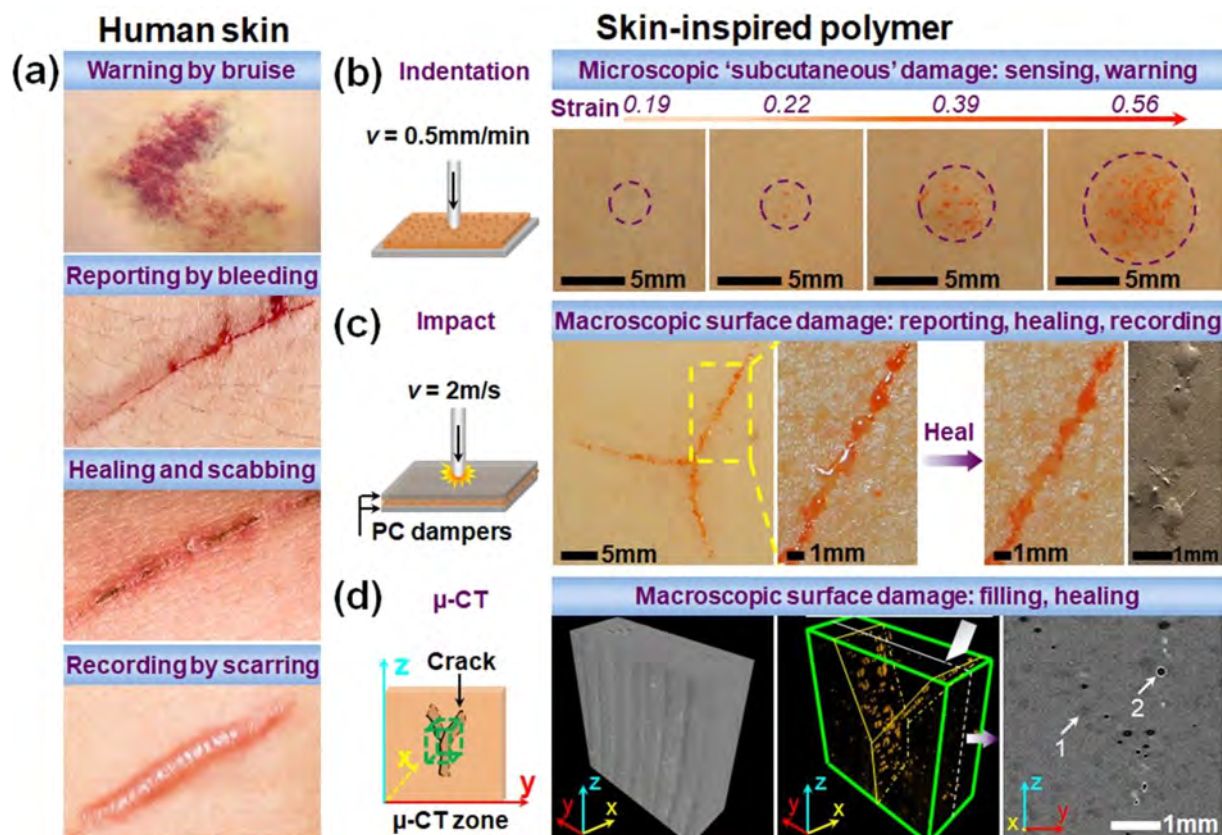


Figure 2. Skin-inspired fully autonomous polymeric material. (a) Response of human skin upon subcutaneous and surface injuries.^{39–41} (b) Sensing and warning of microscopic “subcutaneous” damage in the synthetic smart material. (c) Sequential reporting, healing, and recording of microscopic surface damage in smart material. “Bleeding” occurred analogous to human skin. “Scab” stayed on the crack after solidification and turned to permanent “scar” with a permanent color to record healed damage. (d) Healed damage observed via μ -CT, including 3D reconstructed specimen (left), 3D distribution of fractured microcapsules (bright regions) from μ -CT images (middle), and a typical cross-section in y - z plane (right). Arrows 1 and 2 indicate an intact microcapsule and an empty microcapsule, respectively.

encapsulated according to the protocol established by Jin et al.,³⁷ and the obtained corresponding microcapsules were further strengthened using a coating process developed by Sun et al.³⁸ After the strengthening process, the epoxy microcapsules have strength high enough to survive the specimen manufacturing process and more impermeable shell for the better isolation of the encapsulated epoxy mixture from the alkaline surroundings (Figure S1).³⁸ Figure 1d shows the appearance of the epoxy microcapsules with a diameter of $235 \pm 57 \mu\text{m}$. Attributed to the reasonable combination of the functional chemicals and the simple carriers in the form of microcapsules, smart materials can be easily fabricated without any modification of the matrices via simply incorporating the dual microcapsules into many damage-sensitive polymeric hosts. In this investigation, smart materials, in the form of epoxy plates with thickness $\sim 2 \text{ mm}$, were fabricated by mixing 5 or 10 wt % of the dual microcapsules at the optimized ratio (1:1) into the host matrix.³⁶

Response to Microscopic “Subcutaneous” Damage.^{39–41} The smart material can sense and warn of microscopic “subcutaneous” damage visualized by color when indented heavily to different strains from 0.16 to 0.56 (Figure 2b, Figure S2 and S3a). It did not fail macroscopically within the applied strains since no detectable force drop occurred during the indentation (Figure S2). Evident red spots were observed in the indented sites soon after indentation (in less than 10 min) with strains larger than 0.22. The color is strain-

sensitive, as it did not appear for strains smaller than 0.19 and had increased intensity and area with the increased strain beyond that value. This phenomenon is analogous to a bruise of human skin upon impact or heavy pressing (Figure 2a). Whereas a bruise in skin is caused by the accumulated blood from fractured capillary vessels, the color in this synthetic material is attributed to the contact of F10B-0.5DCF from the fractured epoxy microcapsules during indentation with the amine around. We measured the nominal failure strain (displacement over diameter, $\Delta l/d$) of the adopted epoxy microcapsules by compressing a single microcapsule (Figure 3a,b). Its lower limit is ~ 0.20 , which is quite close to the threshold strain for appearance of a “bruise” by indentation. The alkaline source for this color change during indentation was identified by indenting a control epoxy plate containing only 10 wt % F10B-0.5DCF microcapsules to different strains (Figure S3b). Although observable for much larger strains (>0.32), the red color appeared very slowly (in hours) and was very light, which can be explained by the low mobility and alkalinity of the residual amine hardener in the host epoxy matrix.³⁰ The result of this control, together with the fast color change for the smart material, indicates that the dominant trigger for the vibrant “bruise” of the smart material is polyamine from the amine microcapsules. Although no macroscopic failure occurred during indentation, some minor damage might be generated in the host matrix accompanied by the fracture of microcapsules, leading to the vulnerability of

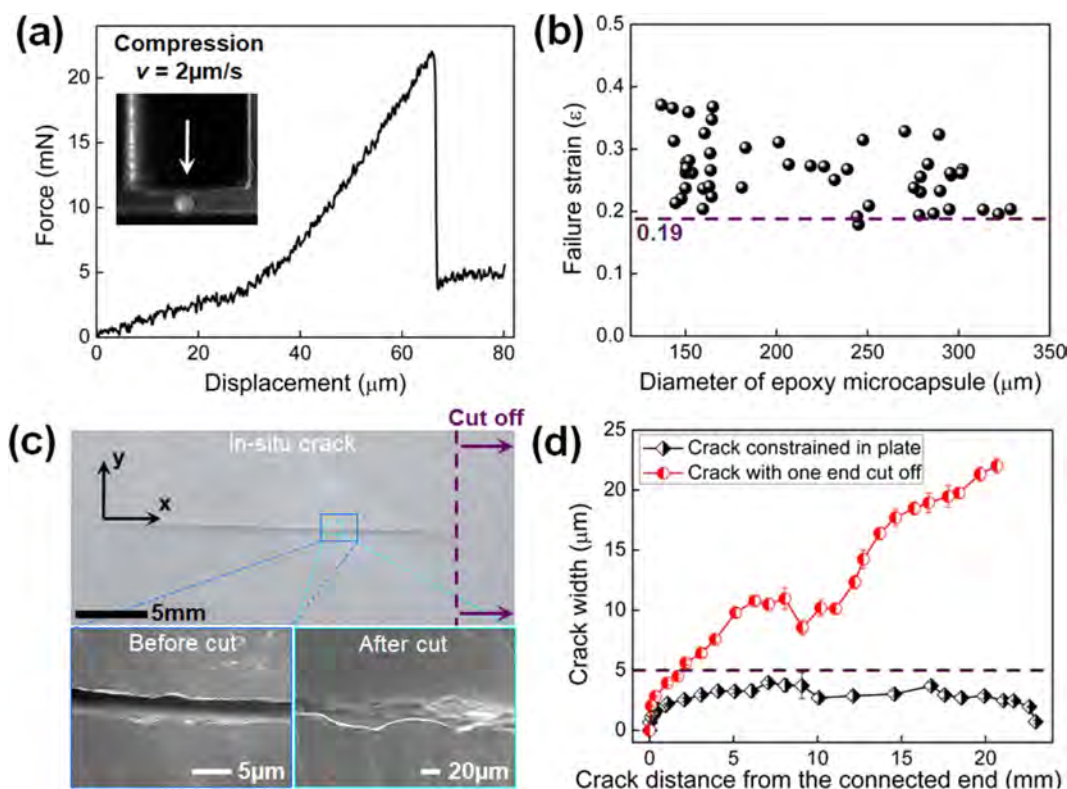


Figure 3. (a) Typical load–displacement curve of a single epoxy microcapsule (293 μm) upon quasi-static compression. (b) Failure strain with respect to the diameter of epoxy microcapsules. (c and d) Width measurement and comparison of a single crack in a neat epoxy plate before and after the removal of constraint from one end by cutting off the joined section.

this area and therefore necessity of early warning. Dissimilar to a bruise of human skin that disappears gradually, the “bruise” in this smart material is stable and permanent to record the experienced damage in the long term.

Response to Macroscopic Surface Damage. Besides microscopic “subcutaneous” damage, macroscopic surface damage in this synthetic smart material can be warned of by visible color immediately after the occurrence (Figure 2c). Herein, in situ cracks were generated controllably by impacting the smart material plate, which is protected by two ductile polycarbonate (PC) dampers, using a drop weight impactor ($v \sim 2\text{ m/s}$). Considering epoxy-based composites are very sensitive to out-of-plane force, autonomous warning of this kind of damage is of practical importance for the application of this smart material. After impact, the cracks turned rapidly to conspicuous red in less than 2 min (Figure S4d). In fact, the time for color change was much shorter than 2 min since it took time for the disassembling of the test specimens and preparation for photographing. We also conducted the same impact test to the control sample with only 10 wt % epoxy microcapsules and compared the color change with respect to damaged time to that of the smart material (Figure S4). Although color appeared gradually with the increased time, analogous to a “bruise”, it was much slower and lighter, which demonstrates the dominant trigger for this type of warning in the smart material is the released polyamine with high mobility and alkalinity from the fractured amine microcapsules.

Filling and subsequent healing of damage by released healants in this smart material were examined via X-ray microcomputed tomography ($\mu\text{-CT}$, Figure 2d) and compared to those of a blank control composed of neat epoxy (Figure S5). For the control, a crack could be clearly distinguished due

to the large density difference between the epoxy matrix ($\sim 1.10\text{ g/cm}^3$) and air in the crack, whereas for the smart material, cracks could be observed in neither the 3D reconstruction nor any cross-section in the y – z plane. Owing to the small density difference between the epoxy matrix and the liquid cores of the two microcapsules ($\sim 0.98\text{ g/cm}^3$ for 25TEPA75T403 and $\sim 1.16\text{ g/cm}^3$ for F10B-0.5DCF), intact microcapsules were only slightly distinguishable (arrow 1 and other dark gray dots in the cross-section). Although the real cracks (left scheme in Figure 2d) were unable to be observed directly by $\mu\text{-CT}$, they could be identified indirectly by the empty microcapsules which were broken by the propagating crack, releasing the healants (arrow 2 and other black dots in the cross-section). 3D distribution of the fractured microcapsules along the cracks was also reconstructed, illustrating that healants, including both the epoxy monomer and polyamine hardener, were extracted out due to the capillary force to fill and subsequently repair the cracks, as quantitatively described hereinafter.

Analogous to human skin, “bleeding” occurred for these in situ cracks (Figure 2c), indicating the released healants far exceeded the required volume to fill the small cracks. Different from cracks in tapered double cantilever beam (TDCB) specimens with constraint only from one end or in tension test specimens without any constraint or self-alignment for self-healing tests,⁴² the in situ crack in the plate is very small attributed to the strong constraint of the matrix. We measured the width of a single crack constrained in a neat epoxy plate using field emission scanning electronic microscopy (FESEM) and compared it to that of the same crack having one end out of the plate by cutting off the joined section at one tip (Figure 3c). The former was smaller than 5 μm , whereas the latter

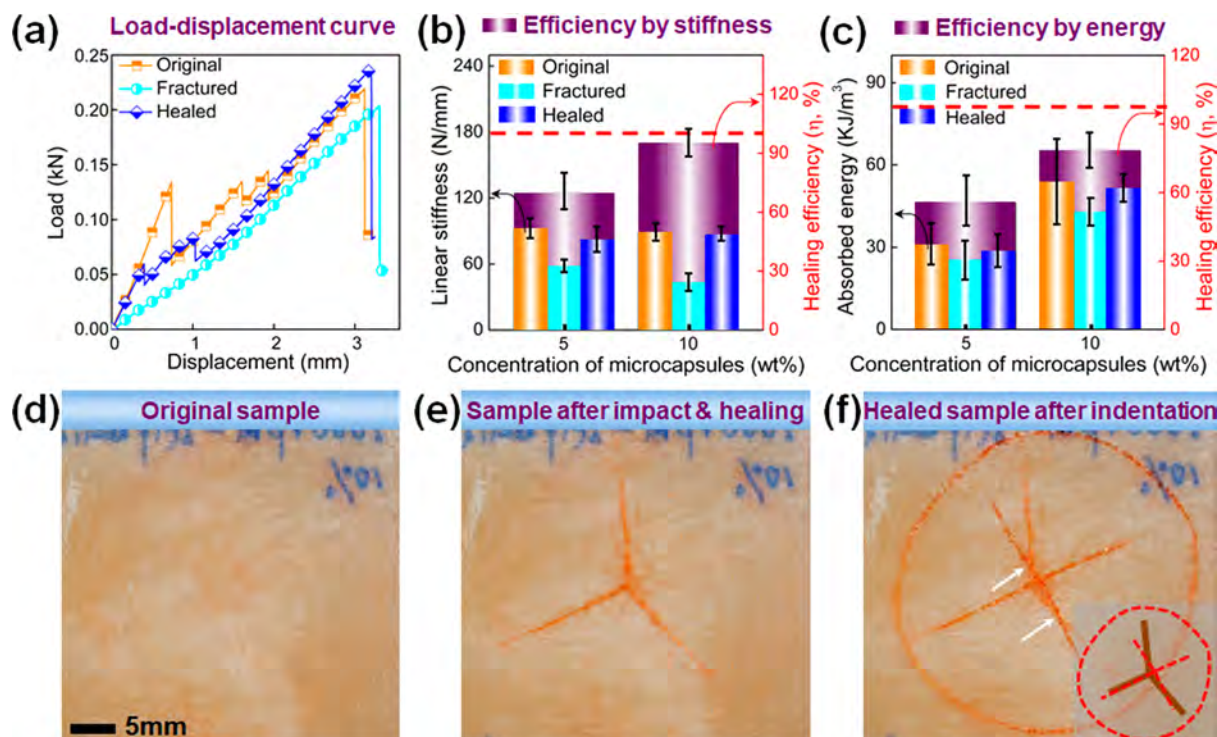


Figure 4. Healing performance of the fully autonomous smart material under dynamic impact damage. (a) Typical load–displacement curves for indentation tests of original specimen, unhealed impacted specimen, and healed specimen. (b and c) Healing efficiency characterized by the recovered structural rigidity and absorbed energy, respectively. (d–f) Original sample, healed impacted sample, and healed sample after indentation, respectively. The two arrows in (f) indicate the new cracks generated during indentation traversed the healed cracks. The circle track is the crack generated along O-ring fixtures during indentation. Inset in (f) shows the healed cracks (brown solid lines) and the newly generated cracks (red dash lines) during indentation. Specimens in (d)–(f) contain a total 10 wt % microcapsules.

gradually increased to more than 20 μm . If the volume of healants that can be released by fractured microcapsules exceeds that of the crack, the material “bleeds” to cover the crack. An inequality about the maximum width of a crack with capability of “bleeding” was deducted (details in the [Supporting Information](#)) and is shown as follows:

$$\bar{t} \leq \frac{\rho_m \bar{d}_1 \omega_1 \psi_1}{\rho_{h1}} + \frac{\rho_m \bar{d}_2 \omega_2 \psi_2}{\rho_{h2}} \quad (1)$$

where \bar{t} is the average width of a crack, ρ_m is the density of the specimen, “1” and “2” mean types of microcapsules, and \bar{d} , ω , ψ , and ρ_h are the average diameter, effective core fraction, concentration of corresponding microcapsule, and density of corresponding healant, respectively. By substituting in the specific values ([Supporting Information](#)), the maximum width of the crack in this smart material could be $\sim 20 \mu\text{m}$, which is much larger than the real width of the in situ crack ($< 5 \mu\text{m}$). This calculation theoretically demonstrates the ability to “bleed” for this smart material.

Healed macroscopic surface damage in this smart material is capable of being recorded stably and permanently by the released healants and color indicator to warn of relatively high vulnerability of the damaged sites even if repaired. After “bleeding”, the liquid on the crack solidified ([Figure 2c](#)), owing to the polymerization of the released healants, to bridge the crack externally, providing extra protection to the crack as a scab would on the cut injury to human skin. Whereas scabs on human skin peel away gradually during the healing process for minor injuries, the “scab” on this smart material stays permanently on the healed crack as a “scar” after solidification

regardless of the severity of damage. Furthermore, due to solidification, the red color is immobilized in the “scab” and the corresponding “scar” thereafter, leading to stable visualization of the healed damage. No evident discolor was observed for the healed specimens aged in the lab for ~ 18 months. This recording of the healed damage, by both permanent “scar” and permanent color, is of practical significance as an early warning to indicate and protect the damaged area as an early warning. It is particularly important for the microcapsule-based systems, since they are one-off systems for both warning and healing functions for the same damaged site.

Thus, through the reasonable combination of functional elements, damage, including microscopic “subcutaneous” damage and macroscopic surface damage, can be warned of in real time after their occurrence and stably and permanently recorded thereafter. It is a comprehensive warning system with rapid and evident response to damage at different levels and stages, which is greatly beneficial to the autonomous life-cycle control of polymeric materials.⁴

Quantification of Autonomous Healing Performance.

Equally important for this smart material to comprehensively warn of damage is the ability to autonomously repair damage without external intervention after the occurrence. The monofunctional healability alone by encapsulated amine–epoxy chemistry has been demonstrated previously with fully autonomous recovery of mode I fracture toughness using the TDCB specimen.³⁶ To reflect healing behavior under a more realistic damaging situation, we tested the recovered properties of this smart material from the dynamic impact damage. To quantitatively characterize the healing performance, we

conducted a quasi-static indentation test on the healed specimen using a protocol similar to compression-after-impact (Figure S6)⁴³ and compared its indentation behavior to those of the original specimen and unhealed damaged specimen (Figure 4a). After being healed at RT for 48 h without external intervention, the specimens behaved more similar to the original specimen during indentation.

Quantitative healing performance in terms of recovered structural rigidity and absorbed energy during indentation is shown in Figure 4b,c, respectively. The healing efficiency was defined in the Experimental Section for this indentation-after-impact protocol. With increasing concentration of microcapsules from 5 wt % to 10 wt %, the recovery of the structural rigidity increased from ~70% to ~95%, while that of the absorbed energy increased from ~55% to ~78%. The reason for the relatively low healing performance by absorbed energy in comparison with that by structural rigidity is that the absorbed energy is a more comprehensive parameter to evaluate the whole indentation process. However, compared to the full recovery of fracture toughness (>100%), healing performance using this protocol is lower, especially regarding the absorbed energy. The relatively low healing performance lies in the fracture behavior of material upon out-of-plane impact and indentation is much more complicated than that upon a quasi-static test using a TDCB specimen. Besides the main crack during impact, other patterns (Figure S7) appeared, including crack branching, secondary cracks, complete abscission of fragments in cracks, and local mis-alignment of the crack surfaces near the impact point. Healing in these areas is weaker, in contrast to the rest of the area with only the main crack.

We also examined the healing behavior by visually checking the tested specimens (Figure 4d–f). For the shown case herein, during indentation one crack initiated and propagated along the healed crack, whereas the other three did not (inset in Figure 4f). In addition, during the growth of these cracks, two of them propagated across, rather than along, the existing healed cracks (arrows in Figure 4f), which indicates these cracks generated during impact were fully repaired and the strength is equal to or even higher than that of the host matrix. After the healing test, the crack surfaces were imaged by FESEM, showing that they were perfectly wet and covered by the released healants due to the good compatibility between the cured healants and the host matrix (Figure S8). Owing to the good healing performance, the shortcoming of microcapsule-based smart materials can be partly compensated as one-off systems.

Validity of the Smart Feature in Other Polymeric Matrices. The smart features based on the dual microcapsules can be easily and readily transplanted to other polymeric materials which are susceptible to damage, since the multifunction carried by the microcapsules is independent of host matrices. For simple demonstrations, the dual microcapsules (10 wt %, 1:1) were mixed into two flexible resins, i.e., NOA 61 based on a UV-curable polyester and Humiseal UV40 based on a UV-curable acrylated polyurethane. Vibrant red color can be observed for incision damage after the specimens were manually cut by a sharp blade (Figure S9a,c). In stark contrast, these two UV-curable resins with only 10 wt % F10B-0.5DCF microcapsules were incapable of visualizing the damage due to lack of the amine trigger (Figure S9b,d). The two examples verify not only the versatility of this smart system in other damage-sensitive polymeric materials but also the effectiveness

of the system for damage in other forms caused by different conditions.

CONCLUSIONS

In summary, we have demonstrated the development of a smart material that functionally mimics human skin in terms of warning and repairing damage simultaneously. Through simple addition of reasonably designed dual microcapsules, the material is able to not only rapidly and conspicuously visualize damage at different levels and stages but also fully autonomously repair the damage with high performance up to 100% without any external interventions. The two functions together promote the real-time life-cycle control of materials with enhanced safety and longevity. This smart system is of practical significance since the multifunction carried by the dual microcapsules is independent of the host matrix and can be easily and readily transplanted to other damage-sensitive polymeric materials, such as functional surface coatings and structural composites.

ASSOCIATED CONTENT

Supporting Information

The Supporting Information is available free of charge on the ACS Publications website at DOI: [10.1021/acs.chemmater.9b00398](https://doi.org/10.1021/acs.chemmater.9b00398).

Experiment section, supporting text, supporting figures, supporting tables, and supporting references (PDF)

AUTHOR INFORMATION

Corresponding Authors

*E-mail: zhanghe@scut.edu.cn (H.Z.).

*E-mail: maeyang@ust.hk (J.Y.).

ORCID

He Zhang: 0000-0001-7864-0305

Chenlu Bao: 0000-0002-2956-0103

Fei Duan: 0000-0002-7469-7184

Jinglei Yang: 0000-0002-9413-9016

Author Contributions

J.L.Y. and H.Z. conceived the idea and designed the experiments. J.L.Y. and F.D. supervised the investigation. H.Z. synthesized the materials and carried out most of the experiments. X.Z. conducted the healing test and data analysis using indentation-after-impact protocol. H.Z., X.Z., and X.L. figured out the protocol to generate in situ cracks in the material. C.L.B. helped to improve the encapsulation device and process. K.F. helped to perform the μ -CT tests. All authors have given approval to the final version of the manuscript.

Funding

We thank the SUG from HKUST (R9365) and Hong Kong Research Grants Council (Project No. N_HKUST631/18), the Key Program of National Natural Science Foundation of China (Grant No. 51435005), the National Instrumentation Program (Grant No. 2012YQ230043), the Science and Technology Program of Guangzhou (Grant No. 201607010240), and the Science and Technology Planning Project of Guangdong Province (Grant No. 2015B090904004 and 2018A030313264), for financial support.

Notes

The authors declare no competing financial interest.

ACKNOWLEDGMENTS

We thank M. Periyasamy from NTU for sharing knowledge about generating in situ cracks in material and H. Giertzsch for performing μ -CT tests at the Institute for Composite Materials (IVW GmbH) Germany. We are grateful to Graham Young from MAE of HKUST for the discussion and improvement of the clarity of this work.

REFERENCES

- (1) Caruso, M. M.; Davis, D. A.; Shen, Q.; Odom, S. A.; Sottos, N. R.; White, S. R.; Moore, J. S. Mechanically-Induced Chemical Changes in Polymeric Materials. *Chem. Rev.* **2009**, *109* (11), 5755–5798.
- (2) Shchukin, D.; Möhwald, H. A Coat of Many Functions. *Science* **2013**, *341* (6153), 1458–1459.
- (3) Li, J.; Nagamani, C.; Moore, J. S. Polymer Mechanochemistry: From Destructive to Productive. *Acc. Chem. Res.* **2015**, *48* (8), 2181–2190.
- (4) Patrick, J. F.; Robb, M. J.; Sottos, N. R.; Moore, J. S.; White, S. R. Polymers with autonomous life-cycle control. *Nature* **2016**, *540* (7633), 363–370.
- (5) Huynh, T. P.; Sonar, P.; Haick, H. Advanced Materials for Use in Soft Self-Healing Devices. *Adv. Mater.* **2017**, *29* (19), 1604973.
- (6) Baginska, M.; Blaiszik, B. J.; Merriman, R. J.; Sottos, N. R.; Moore, J. S.; White, S. R. Autonomic Shutdown of Lithium-Ion Batteries Using Thermoresponsive Microspheres. *Adv. Energy Mater.* **2012**, *2* (5), 583–590.
- (7) Ramirez, A. L. B.; Kean, Z. S.; Orlicki, J. A.; Champhekar, M.; Elsagr, S. M.; Krause, W. E.; Craig, S. L. Mechanochemical strengthening of a synthetic polymer in response to typically destructive shear forces. *Nat. Chem.* **2013**, *5* (9), 757–761.
- (8) Wang, C.; Wu, H.; Chen, Z.; McDowell, M. T.; Cui, Y.; Bao, Z. Self-healing chemistry enables the stable operation of silicon microparticle anodes for high-energy lithium-ion batteries. *Nat. Chem.* **2013**, *5*, 1042.
- (9) Chen, Z.; Hsu, P.-C.; Lopez, J.; Li, Y.; To, J. W. F.; Liu, N.; Wang, C.; Andrews, S. C.; Liu, J.; Cui, Y.; Bao, Z. Fast and reversible thermoresponsive polymer switching materials for safer batteries. *Nat. Energy* **2016**, *1*, 15009.
- (10) Zhang, H.; Zhang, X.; Chen, Q.; Li, X.; Wang, P.; Yang, E.-H.; Duan, F.; Gong, X.; Zhang, Z.; Yang, J. Encapsulation of shear thickening fluid as an easy-to-apply impact-resistant material. *J. Mater. Chem. A* **2017**, *5* (43), 22472–22479.
- (11) Davis, D. A.; Hamilton, A.; Yang, J. L.; Cremer, L. D.; Van Gough, D.; Potisek, S. L.; Ong, M. T.; Braun, P. V.; Martinez, T. J.; White, S. R.; Moore, J. S.; Sottos, N. R. Force-induced activation of covalent bonds in mechanoresponsive polymeric materials. *Nature* **2009**, *459* (7243), 68–72.
- (12) Chen, Y.; Spiering, A. J. H.; Karthikeyan, S.; Peters, G. W. M.; Meijer, E. W.; Sijbesma, R. P. Mechanically induced chemiluminescence from polymers incorporating a 1,2-dioxetane unit in the main chain. *Nat. Chem.* **2012**, *4*, 559.
- (13) Peterson, G. I.; Larsen, M. B.; Ganter, M. A.; Storti, D. W.; Boydston, A. J. 3D-Printed Mechanochromic Materials. *ACS Appl. Mater. Interfaces* **2015**, *7* (1), 577–583.
- (14) Lowe, C.; Weder, C. Oligo(p-phenylene vinylene) excimers as molecular probes: Deformation-induced color changes in photoluminescent polymer blends. *Adv. Mater.* **2002**, *14* (22), 1625–1629.
- (15) Robb, M. J.; Li, W.; Gergely, R. C. R.; Matthews, C. C.; White, S. R.; Sottos, N. R.; Moore, J. S. A Robust Damage-Reporting Strategy for Polymeric Materials Enabled by Aggregation-Induced Emission. *ACS Cent. Sci.* **2016**, *2* (9), 598–603.
- (16) Lee, T. H.; Song, Y. K.; Park, S. H.; Park, Y. I.; Noh, S. M.; Kim, J. C. Dual stimuli responsive self-reporting material for chemical reservoir coating. *Appl. Surf. Sci.* **2018**, *434*, 1327–1335.
- (17) Rifaie-Graham, O.; Apebende, E. A.; Bast, L. K.; Bruns, N. Self-Reporting Fiber-Reinforced Composites That Mimic the Ability of Biological Materials to Sense and Report Damage. *Adv. Mater.* **2018**, *30* (19), 1705483.
- (18) White, S. R.; Sottos, N. R.; Geubelle, P. H.; Moore, J. S.; Kessler, M. R.; Sriram, S. R.; Brown, E. N.; Viswanathan, S. Autonomic healing of polymer composites. *Nature* **2001**, *409* (6822), 794–797.
- (19) Chen, X. X.; Dam, M. A.; Ono, K.; Mal, A.; Shen, H. B.; Nutt, S. R.; Sheran, K.; Wudl, F. A thermally re-mendable cross-linked polymeric material. *Science* **2002**, *295* (5560), 1698–1702.
- (20) Theriault, D.; White, S. R.; Lewis, J. A. Chaotic mixing in three-dimensional microvascular networks fabricated by direct-write assembly. *Nat. Mater.* **2003**, *2* (4), 265–271.
- (21) Cordier, P.; Tournilhac, F.; Soulie-Ziakovic, C.; Leibler, L. Self-healing and thermoreversible rubber from supramolecular assembly. *Nature* **2008**, *451* (7181), 977–980.
- (22) Ghosh, B.; Urban, M. W. Self-Repairing Oxetane-Substituted Chitosan Polyurethane Networks. *Science* **2009**, *323* (5920), 1458–1460.
- (23) Burnworth, M.; Tang, L. M.; Kumpfer, J. R.; Duncan, A. J.; Beyer, F. L.; Fiore, G. L.; Rowan, S. J.; Weder, C. Optically healable supramolecular polymers. *Nature* **2011**, *472* (7343), 334–337.
- (24) Norris, C. J.; Meadway, G. J.; O'Sullivan, M. J.; Bond, I. P.; Trask, R. S. Self-Healing Fibre Reinforced Composites via a Bioinspired Vasculature. *Adv. Funct. Mater.* **2011**, *21* (19), 3624–3633.
- (25) Esser-Kahn, A. P.; Thakre, P. R.; Dong, H.; Patrick, J. F.; Vlasko-Vlasov, V. K.; Sottos, N. R.; Moore, J. S.; White, S. R. Three-Dimensional Microvascular Fiber-Reinforced Composites. *Adv. Mater.* **2011**, *23* (32), 3654–3658.
- (26) White, S. R.; Moore, J. S.; Sottos, N. R.; Krull, B. P.; Santa Cruz, W. A.; Gergely, R. C. R. Restoration of Large Damage Volumes in Polymers. *Science* **2014**, *344* (6184), 620–623.
- (27) Patrick, J. F.; Hart, K. R.; Krull, B. P.; Diesendruck, C. E.; Moore, J. S.; White, S. R.; Sottos, N. R. Continuous Self-Healing Life Cycle in Vascularized Structural Composites. *Adv. Mater.* **2014**, *26* (25), 4302–4308.
- (28) Pang, J. W. C.; Bond, I. P. 'Bleeding composites' - damage detection and self-repair using a biomimetic approach. *Composites, Part A* **2005**, *36* (2), 183–188.
- (29) Kling, S.; Czigány, T. Damage detection and self-repair in hollow glass fiber fabric-reinforced epoxy composites via fiber filling. *Compos. Sci. Technol.* **2014**, *99*, 82–88.
- (30) Li, W.; Matthews, C. C.; Yang, K.; Odarczenko, M. T.; White, S. R.; Sottos, N. R. Damage Detection: Autonomous Indication of Mechanical Damage in Polymeric Coatings. *Adv. Mater.* **2016**, *28* (11), 2275–2275.
- (31) Guo, Y. K.; Chen, L.; Xu, D. G.; Zhong, J. R.; Yue, G. Z.; Astruc, D.; Shuai, M. B.; Zhao, P. X. A dual functional epoxy material with autonomous damage indication and self-healing. *RSC Adv.* **2016**, *6* (69), 65067–65071.
- (32) Song, Y. K.; Kim, B.; Lee, T. H.; Kim, J. C.; Nam, J. H.; Noh, S. M.; Park, Y. I. Fluorescence Detection of Microcapsule-Type Self-Healing, Based on Aggregation-Induced Emission. *Macromol. Rapid Commun.* **2017**, *38* (6), 1600657.
- (33) Hu, M. H.; Peil, S.; Xing, Y. W.; Dohler, D.; Caire da Silva, L.; Binder, W. H.; Kappl, M.; Bannwarth, M. B. Monitoring crack appearance and healing in coatings with damage self-reporting nanocapsules. *Mater. Horiz.* **2018**, *5* (1), 51–58.
- (34) Wang, J.-P.; Wang, J.-K.; Zhou, Q.; Li, Z.; Han, Y.; Song, Y.; Yang, S.; Song, X.; Qi, T.; Möhwald, H.; Shchukin, D.; Li, G. L. Adaptive Polymeric Coatings with Self-Reporting and Self-Healing Dual Functions from Porous Core-Shell Nanostructures. *Macromol. Mater. Eng.* **2018**, *303* (4), 1700616.
- (35) Pu, W.; Fu, D.; Wang, Z.; Gan, X.; Lu, X.; Yang, L.; Xia, H. Realizing Crack Diagnosing and Self-Healing by Electricity with a Dynamic Crosslinked Flexible Polyurethane Composite. *Adv. Sci.* **2018**, *5* (5), 1800101.
- (36) Zhang, H.; Zhang, X.; Bao, C.; Li, X.; Sun, D.; Duan, F.; Friedrich, K.; Yang, J. Direct microencapsulation of pure polyamine

by integrating microfluidic emulsion and interfacial polymerization for practical self-healing materials. *J. Mater. Chem. A* **2018**, *6*, 24092–24099.

(37) Jin, H. H.; Mangun, C. L.; Stradley, D. S.; Moore, J. S.; Sottos, N. R.; White, S. R. Self-healing thermoset using encapsulated epoxy-amine healing chemistry. *Polymer* **2012**, *53* (2), 581–587.

(38) Sun, D.; Chong, Y. B.; Chen, K.; Yang, J. Chemically and thermally stable isocyanate microcapsules having good self-healing and self-lubricating performances. *Chem. Eng. J.* **2018**, *346*, 289–297.

(39) Lukianova, N. Bruise Close-up photo. In <https://www.alamy.com/bruise-close-up-photo-image229158007.html>. Alamy Inc.: Alamy Stock Photo, 2011, 1630 × 1328 px.

(40) Rueangkham, W. A close up shot photo of lesion on arm, Selective focus, Soft focus. In <https://www.alamy.com/a-close-up-shot-photo-of-lesion-on-arm-selective-focus-soft-focus-image178195559.html>. Alamy Inc.: Alamy Stock Photo., 2018, 3078 × 2052 px.

(41) Marazzi, P. Keloid scar from a cat scratch. In <https://www.sciencephoto.com/media/152813/view/keloid-scar-from-a-cat-scratch>. Sciencephotolibrary, 2011, 5150 × 3421 px.

(42) Takeda, K.; Unno, H.; Zhang, M. Polymer reaction in polycarbonate with Na₂CO₃. *J. Appl. Polym. Sci.* **2004**, *93* (2), 920–926.

(43) Yin, T.; Rong, M. Z.; Wu, J.; Chen, H.; Zhang, M. Q. Healing of impact damage in woven glass fabric reinforced epoxy composites. *Composites, Part A* **2008**, *39* (9), 1479–1487.